Biointerface Research in Applied Chemistry
Platinum Open Access Journal (ISSN: 2069-5837)

*Article*
**Volume 12, Issue 2, 2022, 1856 - 1869**
https://doi.org/10.33263/BRIAC122.18561869

# Apoptotic Cell Death Induction Through Pectin, Guar Gum and Zinc Oxide Nanocomposite in A549 Lung Adenocarcinomas

**Indu Hira [1,†], Reena Kumari [1,†], Adesh Kumar Saini [2], Henok Gullilat [1], Vipin Saini [3], Anil Kumar Sharma [2], Reena V. Saini [2,*]**

1 School of Biotechnology, Faculty of Applied Sciences and Biotechnology, Shoolini University of Biotechnology and Management Sciences, Solan, Himachal Pradesh, 173229, India; isha1982sahotah@gmail.com (I.H.), reena.sharma011@yahoo.com (R.K.), henoksheba@gmail.com (H.G.);
2 Department of Biotechnology, MMEC, Maharishi Markandeshwar (Deemed to be University), Mullana-Ambala, Haryana 133207, India; sainiade@mmumullana.org (A.K.S.), anibiotech18@gmail.com (A.K.S.);
3 Maharishi Markandeshwar University, MMT, Solan, Himachal Pradesh, 173229, India; vipinsaini31@rediffmail.com (V.S.);
† Equal contributing authors;
* Correspondence: reenavohra10@mmumullana.org; reenavohra10@gmail.com (R.V.S.);

Scopus Author ID 35554038200
**Received: 5.04.2021; Revised: 10.05.2021; Accepted: 14.05.2021; Published: 10.06.2021**

**Abstract:** Previously, we reported the immunostimulatory potential of the nanocomposite prepared from biopolymers (Pectin and Guar gum) and zinc oxide (Pec-gg-ZnO) on human peripheral-blood lymphocytes leading to enhanced anti-cancer immunity. The current study aims to describe the direct anti-cancer potential of Pec-gg-ZnO nanocomposite and the relevant mechanism of cell death induction in human lung carcinomas (A549). The cytotoxicity assay revealed the anti-cancer potential of Pec-gg-ZnO nanocomposite towards A549 cells, cervical adenocarcinoma (HeLa), and prostatic small cell carcinoma (PC-3). The $IC_{50}$ values were 83.67 ± 0.10 µg/ml, 87.25 ± 0.03 µg/ml and 85.95 ± 0.03 µg/ml for A549, HeLa and PC-3 cells, respectively. The nanocomposite's cancer cells' killing capabilities were significantly higher than pectin and guar gum alone. Hemolysis assay revealed that synthesized Pec-gg-ZnO nanocomposite is biocompatible at 2.5 mg/ml. S phase arrest with enhanced sub-G1 (apoptotic cells) population was examined in A549 cells treated with Pec-gg-ZnO nanocomposite. The nanocomposite caused apoptosis of target cells by inducing mitochondrial depolarisation, reactive oxygen species generation, caspase-3 and Poly (ADP-ribose) polymerase 1 (PARP1) activation resulting in DNA fragmentation. Collectively, the current data revealed that Pec-gg-ZnO nanocomposite is a novel polymer-based anti-cancer agent capable of inducing apoptotic pathways in cancer cells.

**Keywords:** anti-cancer; lung cancer; reactive oxygen species; biopolymers; ZnO.



## 1. Introduction

It has been estimated that by 2020, there will be about 12.0 million cancer deaths and about 15.0 million cancer cases will be detected in India alone [1]. The most commonly used treatments are chemotherapy, radiation therapy, and surgery. All these treatments are harmful in which healthy cells are destroyed and are limited due to their side effects [2]. Cancer is the stage when there is a loss of balance between cell death and cell division. Apoptosis is a mechanism to maintain homeostasis, which usually occurs during development and aging.

During apoptosis, cancerous and virally infected cells are removed, and alterations in apoptotic pathways lead to cancer development and growth [3]. Many genes and proteins are involved in modulating cell death pathways; among them, the caspase family plays a vital role. Mitochondrial membrane depolarization amplifies the apoptotic signals by activation of caspases leading to proteolytic cleavage of cellular targets such as Poly (ADP-ribose) polymerase 1 (PARP1) [4, 5].

Nanotechnology can be described as the restructuring of matter in nanoscale dimensions (i.e., less than 100 nm) to yield materials having new properties and functions [6-8]. Nanocomposites are prepared from nanomaterials by combining one or more components to get each constituent's finest properties [9, 10]. Polymer nanocomposites are prepared by combining polymers and inorganic/organic fillers at the nanometres scale with several electrical, mechanical, and optical characteristics [11-13]. Natural polymers are preferred over synthetic polymers because of their biocompatibility, biodegradability, ability to be metabolized, stability, extensive surface area and nontoxic [14, 15]. Several studies on natural biopolymers revealed anti-cancer activities and tumor growth inhibition via polysaccharides by direct toxicity and biocompatibility of the natural polymers [16, 17]. Previously, the synthesis of the pectin, guar gum and zinc oxide (Pec-gg-ZnO) nanocomposite has been reported from our lab. The nanocomposite displayed a size range of 50-70 nm, which enhanced the anti-cancer potential of peripheral blood lymphocytes against human cancer cells [18].

Pectin and its modified forms have successfully displayed antitumor activities towards aggressive and recurring tumors [19, 20]. Folic acid-functionalized guar gum nanoparticles loaded with methotrexate have been used for targeted delivery to colon cancer cells [21]. It has been reported that anti-cancer drugs coated with guar gum and eudragit conjugated curcumin exhibited enhanced oral bioavailability and solubility [22]. It has been reported that ZnO nanoparticles are capable of inducing apoptotic pathways in cancer cells through reactive oxygen species (ROS) production [23-25]. Nano-formulations synthesized by using both inorganic and organic components can induce apoptosis in cancer cells [26, 27].

The detailed method of Pec-gg-ZnO nanocomposite preparation and characterization has been reported earlier [18]. Current studies deal with evaluating the anti-cancer potential of the polymer-based nanocomposite under in vitro conditions. Here, we are describing new anti-cancer nanocomposite and exploring the cell death mechanism mediated through Pec-gg-ZnO nanocomposite. The apoptotic pathways induced by nanocomposite were studied via examining ROS generation, mitochondrial perturbation, cell cycle alterations and, cleavage of caspase-3 and PARP1 leading to DNA fragmentation in A549 lung adenocarcinomas.

## 2. Materials and Methods

### *2.1. Materials.*

Dulbecco's Modified Eagle Medium (DMEM) and Minimum Essential Medium (MEM), Dimethyl Sulphoxide (DMSO), Fetal Bovine Serum (FBS), Phosphate Buffer Saline (PBS), (3-(4, 5- dimethylthiazol-2yl)-2, 5-diphenyltetrazolium bromide (MTT), Propidium Iodide (PI) and Triton X-100 were procured from Himedia (Mumbai, India). Rhodamine123 (Rh123) and 2,7- dichloroflourescin diacetate (DCFDA) were from Sigma Aldrich. 4′,6-diamidino-2-phenylindole (DAPI) from Thermo fisher scientific. Primary antibodies, purified anti-caspase-3, PARP1 (F-2, sc-8007) and alpha-actinin were purchased from Biolegend and Santa Cruz Biotechnology, respectively.

*2.2. Cell culture.*

Lung adenocarcinoma (A549), cervical adenocarcinoma (HeLa) and prostate carcinoma (PC-3) cell lines were procured from the National Centre for Cell Sciences, Pune, India. The cells were cultured in DMEM medium containing 10% heat-inactivated FBS and penicillin/ streptomycin solution (100 units/ml and 100 mg/ml respectively) at 37°C in a humidified, 5% $CO_2$ atmosphere.

*2.3. Preparation and characterization of the nanocomposite.*

The Pec-gg-ZnO nanocomposite was prepared by the nanoprecipitation method. The obtained nanocomposite has a polygonal morphology with a size ranging from 50-70 nm. The nanocomposite preparation and characterization have been published earlier [18].

*2.4. Hemolysis assay.*

The biocompatibility of the biopolymers pectin, guar gum and the nanocomposite was carried out via hemolytic assay. Blood (10 ml) was collected in EDTA-coated vacutainer tubes from healthy human donors after clearance from the Institute Ethics Committee. Blood was centrifuged at 500 x g for 5 min, aspirate plasma. Wash blood cells with 150 mM NaCl solution, mix and centrifuge at 500 x g for 5 min. Then aspirate supernatant and replace it with PBS. The blood cells were then incubated at 37 °C for one hour with various concentrations (0.25, 0.5, 1.0, 2.5 and 5.0 mg/ml) of Pec, gg, Pec-gg-ZnO nanocomposite. PBS and 10% Triton X-100 were taken as negative and positive controls, respectively. The treated blood cells were collected by centrifugation. Then absorbance of the supernatant (100 µl) was recorded at 541 nm using a microplate reader.

$$\text{Haemolysis (\%)} = \frac{\text{OD}_{\text{test sample}} - \text{OD}_{\text{negative control}}}{\text{OD}_{\text{positive control}} - \text{OD}_{\text{negative control}}} \text{ x } 100$$

where, OD positive control represents absorbance for triton X-100 treated cells; OD negative control represents OD for PBS treated cells and the OD test sample denotes absorbance for treated cells.

*2.5. Cell viability and apoptosis assay.*

Cancer cell lines A549, HeLa and PC-3 ($1x10^4$) were cultured in the 96-well plate and allowed to adhere overnight. Cells were then treated with Pec and gg biopolymers and Pec-gg-ZnO at different concentrations (25, 50, 100 and 200 µg/ml) for 24 h, followed by washing with PBS to remove dead. Untreated cells were used as negative control, and Vincristine sulfate (5 µg/ml) treated cells were positive controls. MTT assay was carried out three times in triplicate as described earlier [18]. The percentage of cell death was calculated by using the formula given below:

$$\text{\% Cell death} = \frac{\text{OD}_{\text{control}} - \text{OD}_{\text{sample}}}{\text{OD}_{\text{control}}} \text{ x } 100$$

where, OD control is the absorbance of untreated cells and the OD sample denotes absorbance of treated cells.

*2.6. Analysis of cell cycle arrest.*

A549 cancer cells were plated into the 6-well plate ($1x10^6$) and treated with biopolymers (Pec and gg) and Pec-gg-ZnO at 100 µg/ml for 24 h. The treated cells were washed and trypsinized. The cells were fixed at 4 °C using 70% ethanol followed by propidium iodide staining, and the cell cycle perturbations were analyzed by using a Flow Canto II- flow cytometer [28] at a central facility of Post Graduate Institute of Medical Education and Research, Chandigarh, India.

*2.7. Measurement of mitochondrial membrane potential.*

A549 cells ($5x10^4$) were incubated for 30 min with biopolymers (Pec and gg) and nanocomposite at 100 µg/ml. After washing, treated cells were collected by trypsinization. Further, cells were stained with Rh 123 (25 µM) in the dark for another 20 min, followed by washing. The mitochondrial membrane depolarization (ΔΨm) was analyzed using a spectrofluorometer having an excitation and emission spectra of 507 and 534 nm, respectively [29]. Vincristine sulfate and Sodium azide were employed as positive controls and untreated cells were used as a negative control.

*2.8. Determination of reactive oxygen species.*

A549 cancer cells ($5 \times 10^4$) were treated for 30 min with biopolymers (Pec and gg) and Pec-gg-ZnO (100 µg/ml), followed by washing and staining with DCFDA in the dark for another 20 min. ROS generation was determined by a spectrofluorometer using excitation and emission spectra of 485 and 530 nm, respectively. Vincristine sulfate and H2O2 were worked as positive controls and untreated cells were used as a negative control [30].

*2.9. Analysis of Caspase-3 and PARP 1 activation.*

Caspase-3 activation was detected in untreated A549 cells, vincristine sulphate (positive control), Pec, gg and Pec-gg-ZnO nanocomposite treated cancer cells via western blotting after 24 h of incubation. Cell pellets ($1x10^6$) were lysed with RIPA lysing buffer (1M Tris pH 8.0, 0.5 M EDTA, 8.0, 1 % NP-40, 1 % SDS, 150 mM sodium chloride, 0.5 % sodium deoxycholate and protease inhibitor). Cell lysates (20 µg) were electrophoresed in 15% SDS polyacrylamide gel (12% gel for PARP 1 analysis) and then transferred onto the PVDF membrane. After that the membrane was treated with 5% condensed milk for 1 h. Following washing, the membrane was treated with an anti-caspase-3 antibody (1:1000) or with PARP1 (F-2) antibody (1:1000) at 4 °C overnight. Further membranes were treated with Horseradish peroxidase-tagged anti-mouse antibody at 1:5000 dilutions for 1h. Signals were developed by using an enhanced chemiluminescence detection reagent.

*2.10. Morphological assessment of apoptotic cells by using DAPI staining.*

A549 cells ($5 \text{ X } 10^4$) were treated for 24 h with biopolymers (Pec and gg) and Pec-gg-ZnO (100 µg/ml) for 24 h. Vincristine sulfate was employed as a positive control. After PBS, washing cells were fixed for 15 min with 4% paraformaldehyde. Followed by treatment with 0.1% Triton X-100 for another 15 min and stained with DAPI in the dark for a further 20 min. The nuclear morphological changes were viewed under a fluorescence microscope (20X) (Olympus 1X 51) after washing the samples with PBS [31].

*2.11. DNA fragmentation assay.*

A549 cells were treated with biopolymers (Pec and gg) and Pec-gg-ZnO (100 µg/ml) for 24 h. The lysis buffer ( 50 mM Tris, 20 mM EDTA, 0.5% Triton X-100) was used to prepare the lysate. The cell lysate was cleared by centrifugation (11,000 rpm, 20 min) and the clear supernatant was subjected to 1% sodium dodecyl sulfate (SDS) and RNase A (0.1mg/ml) for 1 hr at 37 ºC, and then proteinase K treatment was given for 2 h at 56 ºC. For DNA isolation from the supernatant, phenol: chloroform: isoamyl alcohol (25:24:1, v/v/v) was used and an equal volume of isopropanol was utilized for DNA precipitation at -20 ºC. DNA fragmentation was visualized on 1.8% agarose gel with an ultraviolet gel documentation system. [32].

*2.12. Statistical analysis.*

The data were statistically analyzed by using Graph Pad Prism version 6.0. The data was significant when $p \leq 0.05$ and was presented as the average ± standard deviation.

## 3. Results and Discussion

*3.1. Cytotoxicity assessment by hemolysis assay.*

The initial evaluation of the biocompatibility of biopolymers (Pec and gg) and Pec-gg-ZnO nanocomposite was performed via RBC lysis assay. The results are given in Table 1. Pec-gg-ZnO nanocomposite showed overall less hemolysis as compared to Pec and gg. As 5% hemolysis is acceptable for biomaterials; therefore, Pec-gg-ZnO nanocomposite can be considered biocompatible nano-formulation up to a concentration of 2.5 mg/ml (3.389 ± 0.07 % hemolysis).

**Table 1.** Hemolytic analysis after treatment with biopolymers and Pec-gg- ZnO nanocomposite at a concentration range of 0.25 mg/ml to 5 mg/ml for 90 min. Data are presented here as mean ± standard deviation and the experiment was conducted three times.

| Sample | Concentration (mg/ml) | % of Hemolysis |
|---|---|---|
| Phosphate Buffer Saline (PBS) | | 0.047 ± 0.00 |
| Triton X-100 | | 100 |
| Pec | 0.25 | 3.646 ± 0.07 |
| | 0.5 | 3.852 ± 0.07 |
| | 1.0 | 3.390 ± 0.00 |
| | 2.5 | 4.777 ± 0.00 |
| | 5.0 | 5.367 ± 0.03 |
| gg | 0.25 | 2.979 ± 0.00 |
| | 0.5 | 3.081 ± 0.07 |
| | 1.0 | 4.674 ± 0.00 |
| | 2.5 | 3.878 ± 0.10 |
| | 5.0 | 5.187 ± 0.07 |
| Pec-gg-ZnO | 0.25 | 2.028 ± 0.03 |
| | 0.5 | 2.542 ± 0.03 |
| | 1.0 | 2.824 ± 0.07 |
| | 2.5 | 3.389 ± 0.07 |
| | 5.0 | 5.084 ± 0.07 |

*3.2. Pec-gg-ZnO characterization by TEM.*

As described earlier, the size of nanocomposite ranges from 50-70 nm [18]. TEM images showed Pec-gg-ZnO nanocomposite with ZnO embedded in the biopolymer matrix (Figure 1).

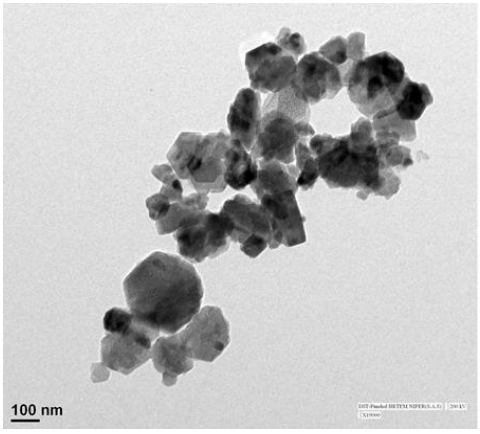


**Figure 1.** TEM analysis of Pec-gg-ZnO showing ZnO (black spots) embedded in the Pec and gg matrices (grey part).

*3.3. Cytotoxicity of Pec-gg-ZnO towards cancer cells.*

The MTT assay revealed the anti-cancer potential of nanocomposite enhanced with an increase in concentrations (25-200 µg/ml) (Figure 2a, b and c). The Pec-gg-ZnO exhibited enhanced cancer cell killing as compared to biopolymers (pec and gg) used alone. $IC_{50}$ values revealed that Pec-gg-ZnO exhibited similar bioactivity towards three cell lines (A549, HeLa and PC-3) used, whereas biopolymers, pec and gg showed very high $IC_{50}$ values towards HeLa cells (Table 2). The $IC_{50}$ values towards A549 and HeLa were undefinable after treatment with pec and gg. Microscopic examination also revealed decreased cell number and altered morphology with the increase in the concentration of the Pec-gg-ZnO (Figure 3).

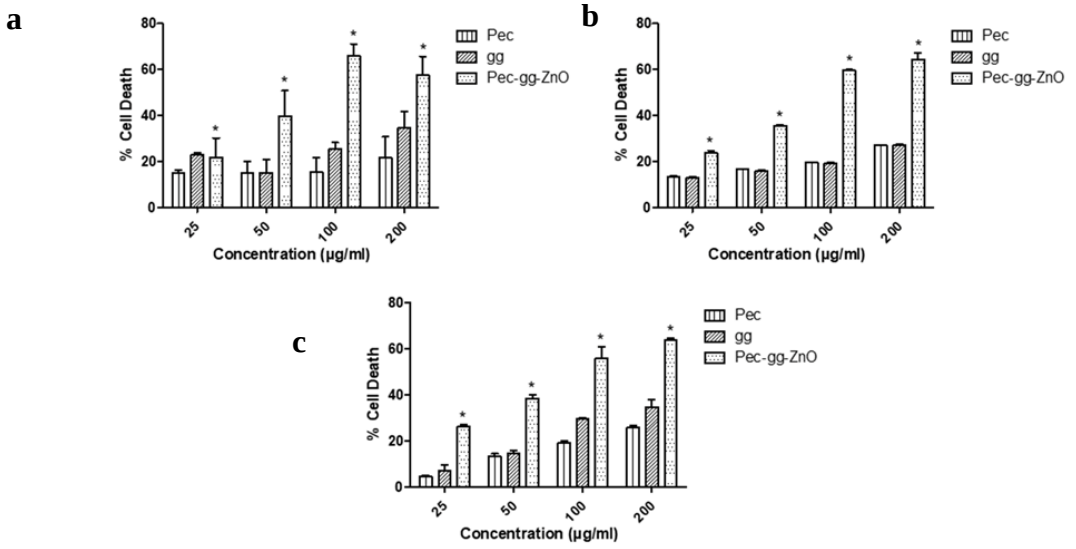


**Figure 2.** Anti-cancer activity of the biopolymers and Pec-gg-ZnO nanocomposite (25-200 µg/ml) after 24 h of exposure on (a) A549 (b) HeLa and (c) PC-3 cancer cells. Data were presented as Mean ± SEM and results were significant as p values is ≤ 0.05 denoted by asterisk (*).

**Table 2**. Comparative analysis of $IC_{50}$ values for A549, HeLa, and PC-3 cells treated with biopolymers (Pec and gg) and Pec-gg-ZnO nanocomposite.

| Cancer cell line | $IC_{50}$ (µg/ml) | | |
|---|---|---|---|
| | **Pec** | **gg** | **Pec-gg-ZnO** |
| A549 | N.A. | N.A. | 83.67±0.10 |
| PC-3 | N.A. | N.A. | 87.25 ±0.03 |
| HeLa | 781.7±0.09 | 374.2±0.08 | 85.95±0.03 |

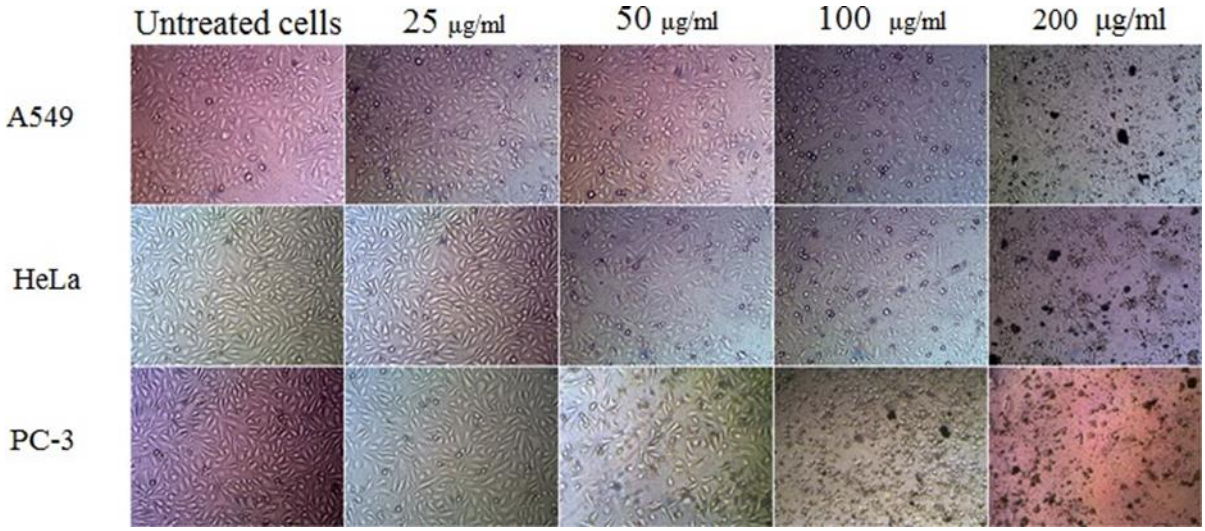


**Figure 3.** Microscopic images of different cell lines (A549, HeLa and PC-3 cells) incubated with Pec-gg-ZnO at various concentrations for 24 h.

*3.4. Analysis of cell cycle arrest.*

Figure 4, shows the cell cycle analysis on A549 ling carcinomas after incubation with biopolymers (Pec and gg) and Pec-gg-ZnO nanocomposite. The results showed cell cycle arrest in S-phase following treatment with biopolymers and Pec-gg-ZnO nanocomposite. Furthermore, Pec-gg-ZnO nanocomposite pre-treated A549 cells displayed significantly (10.35 ± 2.25) enhanced apoptosis (Sub-G1 phase) as compared to negative control (1.75 ± 0.05). Pec and gg-treated A549 cells exhibited a small increase in Sub-G1 stage cells, 1.90 ± 0.08 % and 2.35 ± 1.55 %, respectively.

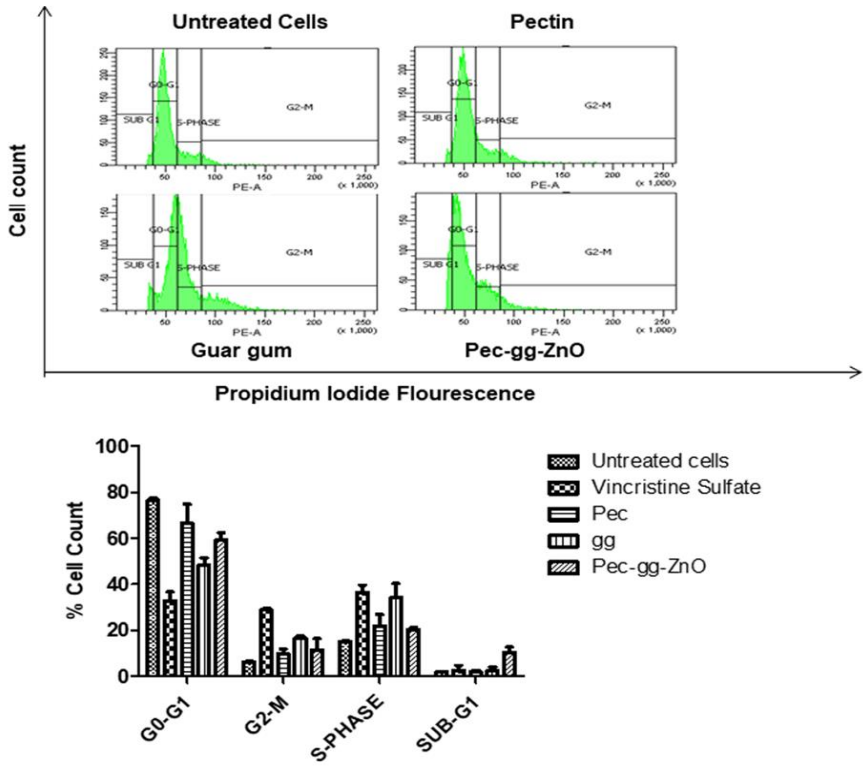


**Figure 4.** Cell cycle phases of A549 cells incubated for 24 h with biopolymers (Pec and gg) and nanocomposite (100 µg/ml). Data were presented as Mean ± S.E.M. of three different experiments and results were significant as p value is ≤ 0.001.

*3.5. Determination of mitochondrial membrane potential.*

Mitochondrial depolarization was evaluated in A549 cancer cells. The results revealed a significant mitochondrial membrane perturbation (Figure 5) when cells were treated with Pec-gg-ZnO nanocomposite compared to other treatments given to the A549 cells. As given in Figure 5, the cells incubated with Pec or gg depicted no change in mitochondrial depolarization after 30 minutes of incubation.

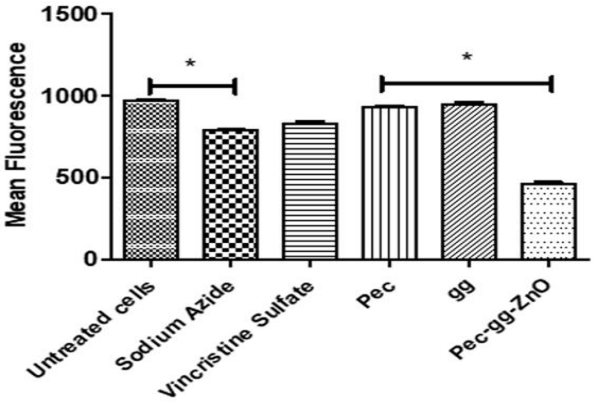


**Figure 5.** Mitochondrial depolarization was analyzed after 30 min. exposure of A549 cells to test samples (100 µg/ml) and controls. The results were shown as Mean ± SEM (n=3 and * $p \leq 0.05$).

*3.6. Intracellular reactive oxygen species generation.*

The generation of ROS by biopolymers (Pec and gg) and Pec-gg-ZnO nanocomposite was assessed by using DCFDA, which detects intracellular H2O2. Pre-treatment with Pec-gg-ZnO nanocomposite caused a 12-fold increase in ROS levels (DCF fluorescence), whereas Pec and gg treated cells displayed 2-fold and 1.8-fold increase in DCF fluorescence, respectively. $H_2O_2$ treated cells were used as positive controls (Figure 6).

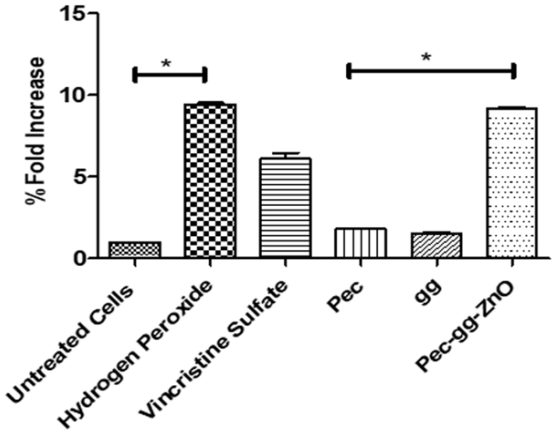


**Figure 6**. ROS generation was analyzed after 30 minutes of exposure of A549 cells to test samples (100 µg/ml) and control (n=3) and expressed here as fold increase in fluorescence. The data was shown here as Mean ± SEM (* $p \leq 0.05$).

*3.7. Caspase-3 and PARP1 activation.*

To evaluate the apoptotic pathway activated by Pec-gg-ZnO nanocomposite, cleaved caspases-3 and PARP1 proteins were analyzed. The data depicted activated caspase-3 in Pec-gg-ZnO treated A549 cells, but Pec and gg did not affect caspase-3 cleavage (Figure 7). Following nanocomposite treatment, the PARP1 cleaved fragment of 24 kDa was detected in

A549 cell lysate, which suggested Pec-gg-ZnO induce cancer cells death by caspase-3 and PARP1 stimulation. Caspase-3 and PARP1 mediated cancer cell death was also evident in vincristine sulfate (positive control) treated cells but not in Pec and gg treated cells (Figure 7).

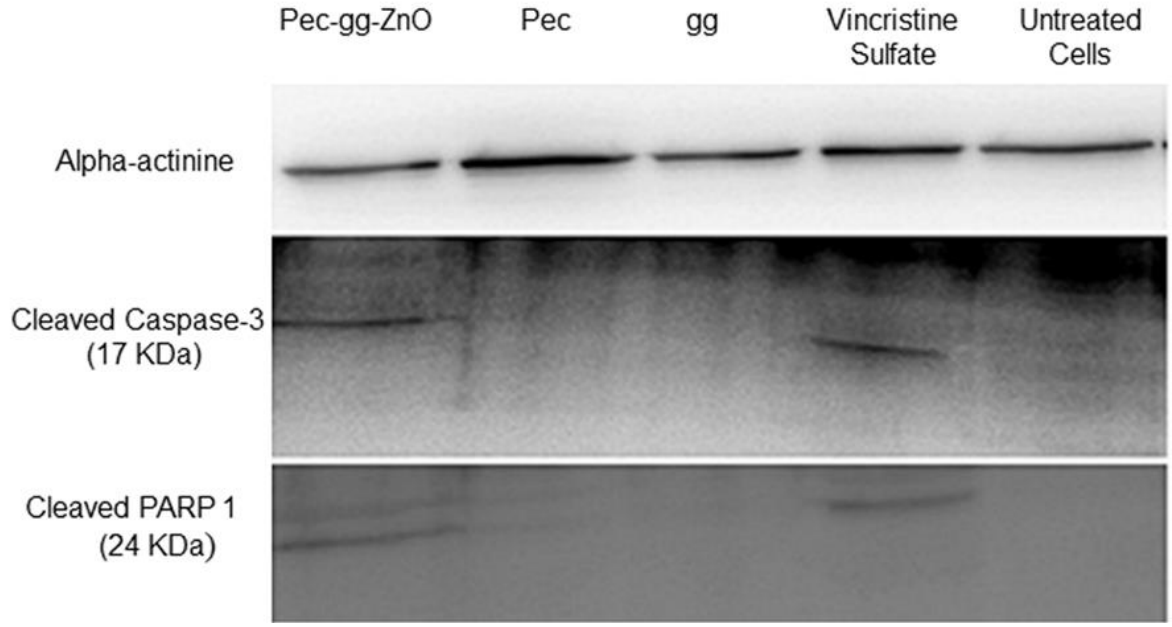


**Figure 7.** Cleaved caspase-3 and PARP 1 in the cellular lysate of A549 cells treated with Pec, gg and Pec-gg-ZnO nanocomposite. Vincristine sulfate treated cells were used as positive and untreated cells as a negative control. The experiment was performed three times.

*3.8. Morphological assessment of apoptotic cells by DAPI staining.*

The morphology of apoptotic cells is characterized by cell shrinkage, nuclear blabbing, DNA fragmentation and chromatin condensation. To check apoptosis in A549 cells were treated with biopolymers (Pec and gg) and Pec-gg-ZnO (100 µg/ml) nanocomposite followed by DAPI staining. Untreated cells, Pec and gg treated cells showed normal nuclei, whereas the cells treated with Pec-gg-ZnO nanocomposite displayed condensed and fragmented nuclei which are characteristics of apoptosis (Figure 8).

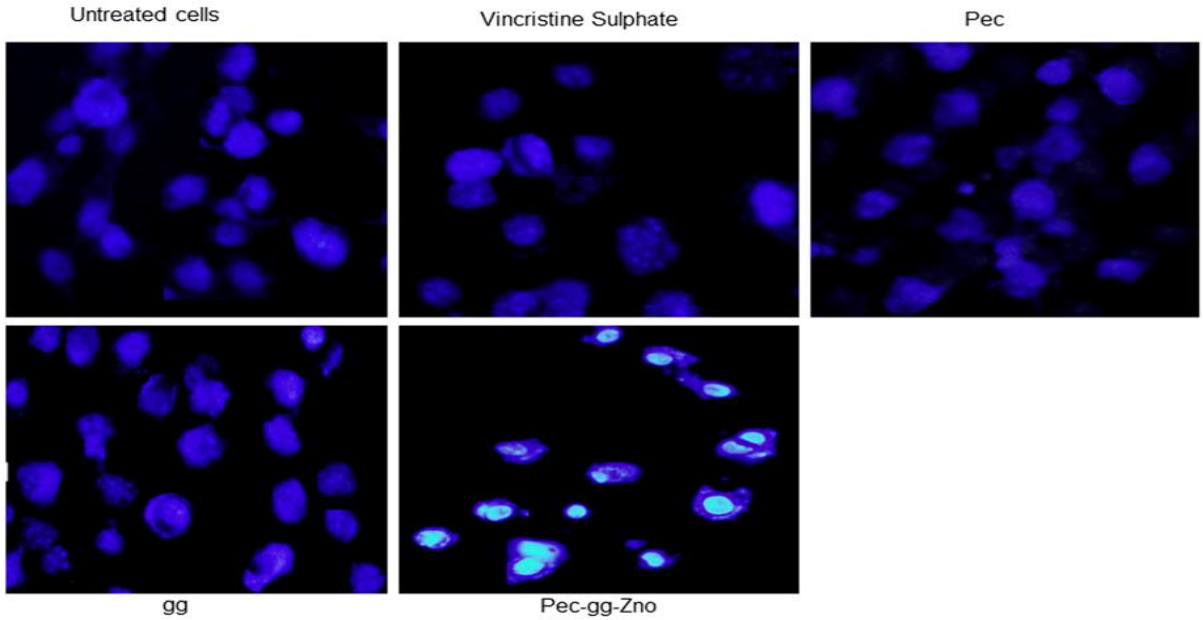


**Figure 8.** Fluorescent microscopic images of DAPI staining.

*3.9. DNA fragmentation analysis.*

Cleavage of genomic DNA into a ladder of small fragments is one of the hallmarks of apoptosis [33]. Pec-gg-ZnO treated A549 cells displayed a typical DNA fragmentation following 24 h of incubation, whereas Pec and gg treated cells did not display any DNA cleavage (Figure 9).

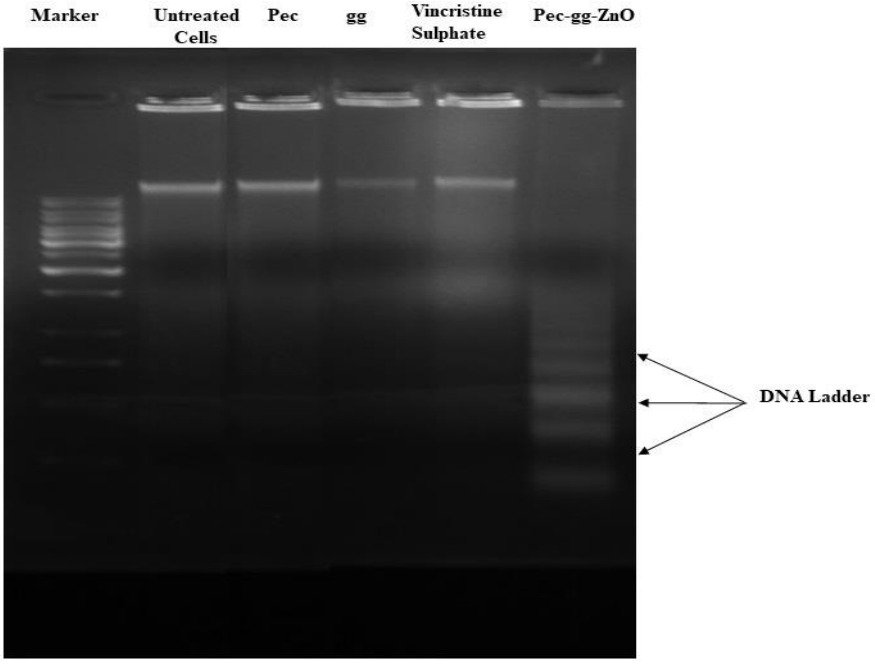


**Figure 9.** DNA fragmentation analysis for apoptosis detection. Pec-gg-ZnO (100 µg/ml) treated cells showed typical DNA fragments.

## 4. Discussion

It has been reported earlier that Pectin extracts inhibit hypotonicity-induced lysis of erythrocyte membrane, thereby exhibiting membrane stabilization effect and were biocompatible [34]. Similarly, it has been shown that guar gum displayed negligible toxicity against the human erythrocyte, revealing biocompatibility of the guar gum [35]. The data here also revealed the biocompatibility of biopolymers (Pec and gg) and the nanocomposite at 2.5 mg/ml, which suggests minimal toxicity of nanocomposite even at higher concentrations.

Pec-gg-ZnO nanocomposite exhibited anti-cancer activity towards A549, HeLa and PC-3 cells. Earlier, heat-modified Citrus pectin has been shown to induce cell death in HepG2 and A549 cells through the process of autophagy [36]. Guar seeds extract been shown to possess anti-cancer potential towards PC-3 and human colorectal carcinomas (HCT116 and CACO-2) [37]. The enhanced cancer cell death via Pec-gg-ZnO suggested that the interaction between Pec, gg and ZnO at the nano level has enabled the Pec-gg-ZnO formulation mediated cancer cell death under in vitro conditions.

One of the hallmarks of cancer is uncontrolled cell division [38] and inhibition of the cell cycle progression is considered as a practical approach to eradicate cancer cells [39]. Cell cycle analysis showed that Pec-gg-ZnO nanocomposite induced S phase arrest leading to apoptotic of cancer cells. Mitochondrial dysfunction has been shown to play a central role in apoptotic induction [40, 41]. Similarly, elevation in ROS levels causes cancer cell death selectively without affecting normal cells. N-ethyl-4-(2-isothiocyanatoethyl) benzamide (LBL21) is a ROS-modulating agent which resulted in the anti-cancer activity of LBL21

towards stem-like cancer cells and mice bearing A549 lung cancer xenografts [42]. The current data indicated that the Pec-gg-ZnO nanocomposite caused mitochondrial damage and ROS-mediated killing of cancer cells [43]. Earlier studies have shown that a minor increase in ROS can induce cell proliferation, whereas a significant increase in ROS enhances apoptosis in prostate cancer cells [44]. ZnO NPs have been shown to enhance intracellular ROS levels up to 30–40%, which led to apoptosis induction in human pulmonary adenocarcinoma cells [45]. Pec-gg-ZnO has been shown to activate caspase-3 and PARP1. The downstream activation of various cytoplasmic or nuclear proteins, including PARP, is initiated by activating effector caspases such as caspase-3 [46]. PARP1 is one of the well-known cellular substrates of caspases, which is a distinct feature of apoptosis. In apoptosis, PARP1 (116 kDa) is cleaved by activated caspases-3 into two fragments of 89 kDa and 24 kDa, resulting in the activation of its catalytic activity [47].

## 5. Conclusions

The current study deals with the evaluation of the Pec-gg-ZnO nanocomposite as a novel anti-cancer agent. The hemolytic assay confirmed biocompatibility of the nanocomposite and the cytotoxicity assay revealed the promising anti-cancer activity of Pec-gg-ZnO nanocomposite against A549, Hela and PC-3 cancer cells. Cell cycle analysis revealed S-phase arrest and apoptotic induction in A549 cells treated with Pec-gg-ZnO nanocomposite. Further, mitochondrial depolarization, ROS generation and activation of caspase-3 and PARP1 confirmed the commencement of the apoptotic process by Pec-gg-ZnO nanocomposite. Taken together, the data suggest that Pec-gg-ZnO nanocomposite can be utilized as an anti-cancer therapeutic.

## Funding

The authors are thankful to Maharishi Markandeshwar (Deemed to be University) and Centre of Research on Himalayan Sustainability and Development, Shoolini University, for providing facilities and financial support.

## Acknowledgments

This research has no acknowledgments.

## Conflict of interest

The author declares no conflict of interest in publishing this manuscript.

## References

1. Mallath, M.K.; Taylor, D.G.; Badwe, R.A.; Rath, G.K.; Shanta, V.; Pramesh, C.S.; Digumarti, R.; Sebastian, P.; Borthakur, B.B.; Kalwar, A.; Kapoor, S.; Kumar, S.; Gill, J. G.; Kuriakose, Malhotra, H.; Sharma, S.C.; Shukla, S.; Viswanath, L.; Chacko, R.T.; Pautu, J.L.; Reddy, K.S.; Sharma, K.S.; Purushotham, A.D.; Sullivan, R. The growing burden of cancer in India: epidemiology and social context. *Lancet Oncol.* **2014**, *15*, e205-e212, https://doi.org/10.1016/S1470-2045(14)70115-9.
2. Vaid, P.; Raizada, P.; Saini, A.K.; Saini R.V. Biogenic silver, gold and copper nanoparticles - A sustainable green chemistry approach for cancer therapy. *Sustain. Chem. Pharm.* **2020**, *16*, 100247, https://doi.org/10.1016/j.scp.2020.100247.

3. Baig, S.; Seevasant, I.; Mohamad, J.; Mukheem, A.; Huri, H.Z.; Kamarul, T. Potential of apoptotic pathway targeted cancer therapeutic research: Where do we stand? *Cell Death Dis.* **2016**, *7*, e205, https://doi.org/10.1038/cddis.2015.275.
4. Tang, D.; Kang, R.; Berghe, T.V.; Vandenabeele, P.; Kroemer, G. The molecular machinery of regulated cell death. *Cell Res.* **2019**, *29*, 347-364, https://doi.org/10.1038/s41422-019-0164-5.
5. Decker, P.; Muller, S. Modulating poly (ADP-ribose) polymerase activity: potential for the prevention and therapy of pathogenic situations involving DNA damage and oxidative stress. *Curr. Pharm. Biotechnol.* **2002**, *3*, 275-283, https://doi.org/10.2174/1389201023378265.
6. Ayodele, A.T.; Valizadeh, A.; Adabi, M.; Esnaashari, S.S.; Madani, F.; Khosravani, M.; Adabi, M. Ultrasound nanobubbles and their applications as theranostic agents in cancer therapy: a review. *Biointerface Res. Appl. Chem.* **2017**, *7*, 2253 - 2262.
7. Zahin, N.; Anwar, R.; Tewari, D.; Kabir, M.T.; Sajid, A.; Mathew, B.; Uddin, M. S.; Aleya, L.; Abdel-Daim, M. M. Nanoparticles and its biomedical applications in health and diseases: special focus on drug delivery. *Environ. Sci. Pollut. Res.* **2020,** *27*, 19151-19168, https://doi.org/10.1007/s11356-019-05211-0.
8. Sharma, G.; Naushad, M.; Thakur, B.; Kumar, A.; Negi, P.; Saini, R.; Chahal, A.; Kumar, A.; Stadler, F.J.; Aqil, U.M.H. Sodium Dodecyl Sulphate-Supported Nanocomposite as Drug Carrier System for Controlled Delivery of Ondansetron. *Int. J. Environ. Res. Public Health* **2018**, *15*, 414, https://doi.org/10.3390/ijerph15030414.
9. Rad, Z.P.; Mokhtari, J.; Abbasi, M. Preparation and characterization of *Calendula officinalis*-loaded PCL/ gum arabic nanocomposite scaffolds for wound healing applications. *Iran Polym. J.* **2018**, *28*, 51-63, https://doi.org/10.1007/s13726-018-0674-x.
10. Gollapudi, V.R; Mallavarapu, U.; Seetha, J.; Duddela, V.; Amara, V.R.; Vatti, C.S; Anumakonda, V. In situ generation of antibacterial bimetallic silver and copper nanocomposites using *Tinospora cordifolia* leaf extract as bio reductant. *Biointerface Res. Appl. Chem.* **2020**, *10*, 5569-5574, https://doi.org/10.33263/BRIAC103.569574.
11. Feldman, D. Polymers and Polymer Nanocomposites for Cancer Therapy. *Appl. sci.* **2019**, *9*, 3899, https://doi.org/10.3390/app9183899.
12. Fu, S.; Sun, Z.; Huang, P.; Li, Y.; Hu, N. Some basic aspects of polymer nanocomposites: A critical review. *Nano Materials Science* **2019**, *1*, 2-30, https://doi.org/10.1016/j.nanoms.2019.02.006.
13. Urbano, B.F.; Mella, C.; Vera, M. Smart polymer nanocomposites: recent advances and perspectives. *J. Chil. Chem. Soc.* **2020,** *65*, 4973-4981, https://www.jcchems.com/index.php/JCCHEMS/article/view/1559.
14. Wong, K.H.; Lu, A.; Chen, X.; Yang, Z. Natural Ingredient-Based Polymeric Nanoparticles for Cancer Treatment. *Molecules* **2020**, *25*, 3620, https://doi.org/10.3390/molecules25163620.
15. Zare, E.N.; Makvandi, P.; Borzacchiello, A.; Tay, F.R.; Ashtari, B.; Padil, V.V.T. Antimicrobial gum bio-based nanocomposites and their industrial and biomedical applications. *Chem. Commun.* **2019**, *55*, 14871-14885, https://doi.org/10.1039/c9cc08207g.
16. Rapa, M.; Stefan, L.M.; Preda, P.; Darie-Nita, R.N.; Gaspar-Pintiliescu, A.; Seciu, A.M.; Vasile, C.; Matei, E.; Predescu, A.M. Effect of hydrolyzed collagen on thermal, mechanical and biological properties of poly (lactic acid) bionanocomposites. *Iran Polym. J.* **2019**, *28*, 271-282, https://doi.org/10.1007/s13726-019-00694-7.
17. Thakur, S.; Saini, R.V.; Singh, P.; Raizada, P.; Thakur, V.K.; Saini, A.K. Nanoparticles as an emerging tool to alter the gene expression: Preparation and conjugation methods. *Mater. Today Chem.* **2020**, *17*, 100295, https://doi.org/10.1016/j.mtchem.2020.100295.
18. Hira, I.; Kumar, A.; Kumari, R.; Saini, A.K.; Saini, R.V. Pectin-guar gum-zinc oxide nanocomposite enhances human lymphocytes cytotoxicity towards lung and breast carcinomas. *Mater. Sci. Eng.* C **2018**, *90*, 494-503, https://doi.org/10.1016/j.msec.2018.04.085.
19. Zaitseva, O.; Khudyakov, A.; Sergushkina, M.; Solomina, O.; Polezhaeva, T. Pectins as a universal medicine. *Fitoterapia* **2020**, *146*, 104676, https://doi.org/10.1016/j.fitote.2020.104676.
20. Leclere, L.; Cutsem, P.V.; Michiels, C. Anti-cancer activities of pH- or heat-modified pectin. *Front. Pharmacol*. **2013**, *4*, 128, https://doi.org/10.3389/fphar.2013.00128.
21. Sharma, M.; Malik, R.; Verma, A.; Dwivedi, P.; Banoth, G.S.; Pandey, N.; Sarkar, J.; Mishra, P.R.; Dwivedi, A.K. Folic acid conjugated guar gum nanoparticles for targeting methotrexate to colon cancer. *J. Biomed. Nanotechnol.* **2013**, *9*, 96-106, https://doi.org/10.1166/jbn.2013.1474.

22. Kumar, V.S.; John, R.; Sabitha, M. Guargum and eudragit coated curcumin liquisolid tablets for colon specific drug delivery. *Int. J. Biol. Macromol.* **2018**, *110*, 318-327, https://doi.org/10.1016/j.ijbiomac.2018.01.082.
23. Srikanth Vallabani, N.V.; Sengupta, S.; Shukla, R.K.; Kumar, A. ZnO nanoparticles-associated mitochondrial stress-induced apoptosis and G2/M arrest in HaCaT cells: a mechanistic approach, *Mutagenesis* **2019**, *34*, 265-277, https://doi.org/10.1093/mutage/gez017.
24. Wiesmann, N.; Tremel, W.; Brieger, J. Zinc oxide nanoparticles for therapeutic purposes in cancer medicine. *J. Mater. Chem. B.* **2020**, *8*, 4973-4989, https://doi.org/10.1039/D0TB00739K.
25. Wang, S.W.; Lee, C.H.; Lin, M.S.; Chi, C.W.; Chen, Y.J.; Wang, G.S.; Liao, K.W.; Chiu, L.P.; Wu, S.H.; Huang, D.M.; Chen, L.; Shen, Y.S. ZnO nanoparticles induced caspase-dependent apoptosis in gingival squamous cell carcinoma through mitochondrial dysfunction and p70S6K signaling pathway. *Int. J. Mol. Sci.* **2020**, *21*, 1612-1628, https://doi.org/10.3390/ijms21051612.
26. Wei, Q. Y.; Xu, Y. M.; Lau, A.T.Y. Recent progress of nanocarrier-based therapy for solid malignancies. *Cancers* **2020**, *12*, 2783, https://doi.org/10.3390/cancers12102783.
27. Fonseca, A.C.; Serra, A.C.; Coelho, J.F.J. Bioabsorbable polymers in cancer therapy: latest developments. *The EPMA J.* **2015**, *6*, 1-18, https://doi.org/10.1186/s13167-015-0045-z.
28. Girek, M.; Kłosiński, K.; Grobelski, B.; Pizzimenti, S.; Cucci, M.A.; Daga, M.; Barrera, G.; Pasieka, Z.; Czarnecka, K.; Szymański, P. Novel tetrahydroacridine derivatives with iodobenzoic moieties induce G0/G1 cell cycle arrest and apoptosis in A549 non-small lung cancer and HT-29 colorectal cancer cells. *Mol. Cell. Biochem.* **2019**, *460*, 123-150, https://doi.org/10.1007/s11010-019-03576-x.
29. Tian, S,; Saravanan, K.; Mothana, R.A.; Ramachandran, G.; Rajivgandhi, G.; Manoharan, N. Anti-cancer activity of biosynthesized silver nanoparticles using *Avicennia marina* against A549 lung cancer cells through ROS/mitochondrial damages. *Saudi J. Biol. Sci.* **2020**, *27*, 3018-3024, https://doi.org/10.1016/j.sjbs.2020.08.029.
30. Wu, D.; Yotnda, P. Production and detection of reactive oxygen species (ROS) in cancers. *J. Vis. Exp.* **2011**, *57*, e3357, https://doi.org/10.3791/3357.
31. Kumari, R.; Saini, A.K.; Chhillar, A.K.; Saini, V.; Saini, R.V. Antitumor effect of bio-fabricated silver nanoparticles towards ehrlich ascites carcinoma. *Biointerface Res. Appl. Chem.* **2021**, *11*, 12958-12972, https://doi.org/10.33263/BRIAC115.1295812972.
32. Kumari, R.; Saini, A.K.; Kumar, A.; Saini, R.V. Apoptosis induction in lung and prostate cancer cells through silver nanoparticles synthesized from *Pinus roxburghii* bioactive fraction. *J. Biol. Inorg. Chem.* **2020,** *25*, 23-37, https://doi.org/10.1007/s00775-019-01729-3.
33. Peitsch, M.C.; Muller, C.; Tschopp, J. DNA fragmentation during apoptosis is caused by frequent single-strand cuts. *Nucleic Acids Res.* **1993**, *21*, 4206-4209, https://doi.org/10.1093/nar/21.18.4206.
34. Sood, N.; Mathu, A. Evaluation of pharmacological activities of pectin extracted from apple and citrus pomace. *Biolife* **2014**, 2, 1203-1217.
35. Bukhari, S.A.; Shahid, M.; Anjum, F.; Rasheed, A.; Munir, H. Purification, fragmentation and characterization of gum from *Cyamopsis tetragonolobus* to enhance its nutraceutical attributes. *Pak. J. agri. sci.* **2014**, *51*, 1059-1068.
36. Leclere, L.; Fransolet, M.; Cote, F.; Cambier, P.; Arnould, T.; Cutsem, P.V.; Michiels, C. Heat-modified citrus pectin induces apoptosis-like cell death and autophagy in HepG2 and A549 cancer cells. *PLOS One* **2015**, *10*, e0115831, https://doi.org/10.1371/journal.pone.0115831.
37. Badr, S.E.; Abdelfattah, M.S.; El-Sayed, S.H.; El-Aziz, A.S.A.; Sakr, D.M. Evaluation of anti-cancer, antimycoplasmal activities and chemical composition of Guar (*Cyamopsis tetragonoloba*) seeds extract. *Res. J. Pharm. Biol. Chem. Sci.* **2014**, *5*, 414-423.
38. Li, X.; Xu, P.; Wang, C.; Xu, N.; Xu, A.; Xu, Y.; Sadahira, T.; Araki, M.; Wada, K.; Matsuura, E.; Watanabe, M.; Zheng, J.; Sun, P.; Huang, P.; Nasy, Y.; Liu, C. Synergistic effects of the immune check point inhibitor CTLA-4 combined with the growth inhibitor lycorine in a mouse model of renal cell carcinoma. *Oncotarget* **2017**, *8*, 21177- 21186, https://doi.org/10.18632/oncotarget.15505.
39. Otto, T.; Sicinski, P. Cell cycle proteins as promising targets in cancer therapy. *Nat. Rev. Cancer.* **2017**, *17*, 93-115, https://doi.org/10.1038/nrc.2016.138.
40. Desagher, S.; Martinou, J-C. Mitochondria as the central control point of apoptosis. *Trends Cell Biol.* **2000**, *10*, 369-377, https://doi.org/10.1016/S0962-8924(00)01803-1.
41. Ly, J.D.; Grubb, D.R.; Lawen, A. The mitochondrial membrane potential (Δψm) in apoptosis; an update. *Apoptosis* **2003**, *8*, 115-128, https://doi.org/10.1023/A:1022945107762.

42. Wang, J.; Luo, B.; Li, X.; Lu, W.; Yang, J.; Hu, Y.; Huang, P.; Wen, S. Inhibition of cancer growth in vitro and in vivo by a novel ROS-modulating agent with ability to eliminate stem-like cancer cells. *Cell Death Dis.* **2017**, *8*, e2887, https://doi.org/10.1038/cddis.2017.272.
43. Trachootham, D.; Alexandre, J.; Huang, P. Targeting cancer cells by ROS-mediated mechanisms: a radical therapeutic approach? *Nat. Rev. Drug Discov.* **2009**, *8*, 579-591, https://doi.org/10.1038/nrd2803.
44. Das, T.P.; Suman, S.; Damodaran, C. Induction of reactive oxygen species generation inhibits epithelial-mesenchymal transition and promotes growth arrest in prostate cancer. *Mol. Carcinog.* **2014**, *53*, 537-547, https://doi.org/10.1002/mc.22014.
45. Wang, C.; Hu, X.; Gao, Y.; Ji, Y. ZnO nanoparticles treatment induces apoptosis by increasing intracellular ROS levels in LTEP-a-2 cells. *Biomed. Res. Int.* **2015**, *2015*, 423287, https://doi.org/10.1155/2015/423287.
46. Huppertz, B.; Frank, H-G.; Kaufmann, P. The apoptosis cascade-morphological and immunohistochemical methods for its visualization. *Anat. Embryol. (Berl).* **1999**, *200*, 1-18, https://doi.org/10.1007/s004290050254.
47. Chaitanya, G.V.; Steven, A.J.; Babu, P.P. PARP-1 cleavage fragments: signatures of cell-death proteases in neurodegeneration. *Cell Commun. Signal* **2010**, *8*, 31, https://doi.org/10.1186/1478-811X-8-31.